Electroporation does not affect human dermal fibroblast proliferation and migration properties directly but indirectly via the secretome

Sara Gouarderes, Layal Doumard, Patricia Vicendo, Anne-Françoise Mingotaud, Marie-Pierre Rols, Laure Gibot

Electroporation does not affect human dermal fibroblast proliferation and migration properties directly but indirectly via the secretome

Sara Gouardères[1], Layal Doumard[1,2], Patricia Vicendo[1], Anne-Françoise Mingotaud[1], Marie-Pierre Rols[2] and Laure Gibot[1,2]*

[1] Laboratoire des IMRCP, Université de Toulouse, CNRS UMR 5623, Université Toulouse III - Paul Sabatier, France

[2] Institut de Pharmacologie et de Biologie Structurale, Université de Toulouse, CNRS, UPS, Toulouse, France

* Correspondence: gibot@chimie.ups-tlse.fr ; Tel.: +33-561556272

Keywords

Electrochemotherapy, gene electrotransfer, wound healing, scratch wound, conditioned medium, bystander effect

Abstract

Aesthetic wound healing is often experienced by patients after electrochemotherapy. We hypothesized that pulsed electric fields applied during electrochemotherapy (ECT) or gene electrotransfer (GET) protocols could stimulate proliferation and migration of human cutaneous cells, as described in protocols for electrostimulation of wound healing. We used videomicroscopy to monitor and quantify in real time primary human dermal fibroblast behavior when exposed *in vitro* to ECT and GET electric parameters, in terms of survival, proliferation and migration in a calibrated scratch wound assay. Distinct electric field intensities were applied to allow gradient in cell electropermeabilization while maintaining reversible permeabilization conditions, in order to mimic *in vivo* heterogeneous electric field distribution of complex tissues. Neither galvanotaxis nor statistical modification of fibroblast migration were observed in a calibrated scratch wound assay after application of ECT and GET parameters. The only effect on proliferation was observed under the strongest GET conditions, which drastically reduced the number of fibroblasts through induction of mitochondrial stress and apoptosis. Finally, we found that 24h-conditioned cell culture medium by electrically stressed fibroblasts tended to increase the migration properties of cells that were not exposed to electric field. RT-qPCR array indicated that several growth factor transcripts were strongly modified after electroporation.

Introduction

When a cell is exposed to an external pulsed electric field, the plasma membrane transiently becomes permeable for ions, hydrophilic drugs and molecules as large as plasmid DNA, which are otherwise unable to penetrate. This spatially and temporally localized physical phenomenon of cell electropermeabilization is named “electroporation” [1,2]. Electroporation has many medical applications [3]. Among them, electrochemotherapy (ECT) [4,5] has reached an established position in local cancer treatment and is the main clinical use of electroporation in human and veterinary medicine. It consists in combining the injection of poorly permeant antitumor drugs, mainly bleomycin or cisplatin, with local application of calibrated electric field pulses to the tumor site. Thus, transient plasma membrane electropermeabilization allows massive penetration of the cytotoxic drugs within the cell, potentiating its antitumor activities. Standardized protocols for ECT treatments have been published in the framework of the European Standard Operating Procedure on Electrochemotherapy (ESOPE) multicenter trial [6]. Interestingly, clinicians commonly observed aesthetic and functional wound healing of the tumor sites treated with electrochemotherapy [7–9]. This clinical outcome of ECT was confirmed by the patients themselves [10], as self-compiled questionnaires underlined an improvement in wound healing, bleeding, aesthetic impairment, and also in activities of daily life and social relations.

Another medical application of electroporation is gene electrotransfer (GET). Gene electrotransfer of plasmid encoding different growth factors is highly promising in cutaneous wound healing [11]. In an *in vivo* wound model, GET of plasmids encoding for example KGF-1 (keratinocyte growth factor) [12], VEGF (Vascular endothelial growth factor) [13], bFGF (fibroblast growth factor) [14] or antimicrobial peptide hCAP-18/LL-37 [15] led to an increased re-epithelialization rate of the wound, collagen synthesis, and angiogenesis. Other studies demonstrated a tendency [16] to a clear [17] beneficial effect of electroporation alone on wound

closure. While standard protocols for acute and chronic wound treatments are limited to antibiotic therapy and wound dressing, innovative therapies like electrostimulation have emerged as alternatives to conventional treatments [18]. Electrostimulation is based on a natural electric process that occurs after wounding. In an intact epidermis, there is an active segregation of Na+ ions owing to the Na+/K+ATPase action and the presence of ENac channels, leading to a sodium gradient from the basal layer of the epidermis to the upper layer [19]. This process creates a transepithelial potential (TEP) within the epidermis. Depending on the body part, this TEP ranges from -10 to -50mV, while its average potential over all sites is -23 mV [20]. After skin damaging, the relocalization of these Na+ ions leads to the creation of an endogenous local electric field of 100 to 200 mV/mm at the wound margins [21,22]. This field plays a major role in wound healing process, particularly through the activation of migration and proliferation of cutaneous cells, as well as the promotion of angiogenesis [23,24].

In this study, we hypothesized that ECT and GET electric parameters could stimulate cutaneous cell migration and proliferation and thus improve the quality of healing after ECT or GET treatment. To investigate this hypothesis, we worked with primary human dermal fibroblasts grown in monolayer. Firstly, classical hallmarks of cell electropermeabilization, viability and death were assessed after exposition to ECT and GET electric parameters. Secondly, we used videomicroscopy to monitor and quantify in real time cell proliferation and cell migration in a calibrated scratch wound assay, two properties that play a major role in cutaneous wound healing process. Because increases in electric conductivity due to electroporation and tissue heterogeneity (cell shape, extracellular matrix…) induce non-uniformity in the electric field distribution within the skin during electroporation, cells located in between the electrodes do not all experience the same field strength *in vivo* [25,26]. For that reason, in this study we decided to scan a wide range of electrical intensity, inducing various degrees of reversible cell electropermeabilization, and check dermal fibroblast proliferation and

migration properties. Finally, the indirect effect of electroporation on cell migration was investigated by cultivating unexposed dermal fibroblasts in 24h-conditioned cell culture medium. An overview of the experimental procedure is presented in schematic 1.

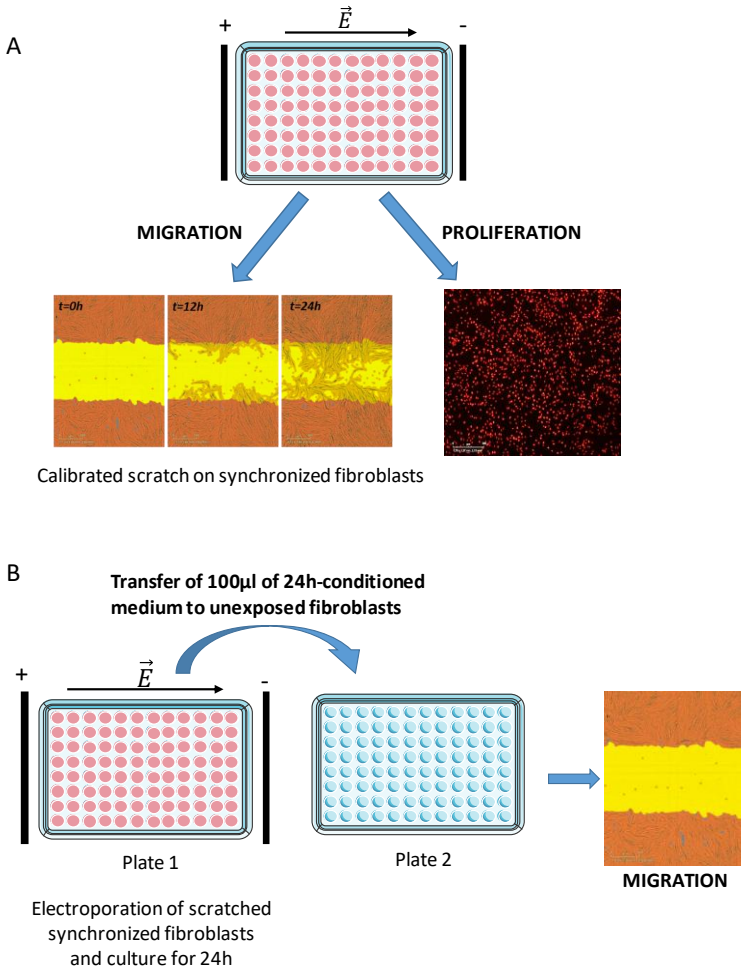

Schematic 1: Overview of the experimental plan to test direct (A) or indirect (B) effects of human dermal fibroblast electroporation on cell behaviour. A. Migration and proliferation properties of fibroblasts submitted to electroporation are followed by videomicroscopy. B. Assessment of indirect effect of electroporation through the secretome. For these experiments, fibroblasts that were not exposed to electric field are cultivated in cell culture medium conditioned for 24h by electroporated fibroblasts. Migration capabilities are then followed by videomicroscopy

Material and methods

Human cutaneous primary cell isolation and cell culture. Primary dermal fibroblasts were isolated from 3-year old foreskin commercially bought (Icelltis) after posthectomy as previously described [27–29]. Cells were tested negative for mycoplasma using MycoAlert mycoplasma detection kit (Lonza) throughout the experiments. Dermal fibroblasts were grown in Dulbecco's Modified Eagles Medium (Gibco-Invitrogen) containing 4.5 $g.L^{-1}$ glucose, Glutamax, and 1mM pyruvate, supplemented with 10 % (v/v) of heat inactivated fetal calf serum, 100 U/ml penicillin, and 100 $\mu g.mL^{-1}$ streptomycin. Cells were maintained at 37°C in a humidified atmosphere containing 5 % CO_2 and cell culture media were changed three times a week.

Electroporation application to cell monolayers. Cells were grown either on gelatin-coated round 1cm glass coverslip [30] or in 96-well plate 24h prior experiments. Cell culture medium was removed from the wells and replaced by 100 µL or 50 µL of pulsing buffer (10 mM K_2HPO_4/KH_2PO_4, 250 mM sucrose, and 1 mM $MgCl_2$ in sterile water, pH 7.4) [31] respectively for glass coverslip or 96-well. Two stainless, flat, parallel electrodes, 1 cm interval (Megastil, Ljubljana, Slovenia) for round coverslip or 0.35 cm interval (Megastil, Ljubljana, Slovenia) for 96-well plates were applied to the bottom of the well. Defined electric field for electrochemotherapy condition (ECT) (8 square-wave pulses of 100 µs, 1 Hz, ranging from 200 to 800 V/cm) and gene electrotransfer (GET) (10 square-wave pulses of 5 ms, 1 Hz, ranging from 50 to 300 V/cm) was delivered at room temperature by Electro cell S20 generator (LeroyBiotech, Saint Orens de Gameville, France). An electric field intensity range was applied in experiments in order to better mimic the heterogeneous distribution of electric field that occurs within vascularized and rich in extracellular matrix tissue such as skin when submitted to electroporation. After electric field application, pulsing buffer was aspired and 200 µL of

fresh cell culture medium were added before cells were placed in a humidified atmosphere at 37°C containing 5% CO_2 until analysis.

Determination of cell electropermeabilization. Plasma membrane electropermeabilization was first assessed through quantification by luminescence of ATP leakage within extracellular medium after cells were submitted to electroporation. For that purpose, cells were grown in 96-well plate and pulsed in 50 µL of pulsation buffer. 10 minutes after electric field application, 40 µL of supernatant was place in white-96-well plate and topped up with 40µl of CellTiterGlo reagent (Promega), incubated for 5 minutes at room temperature and luminescence signal was read on plate reader (Clariostar, BMGLabtech). Secondly, plasma membrane electropermeabilization was assessed by flow cytometry using propidium iodide penetration. Propidium iodide is a non-permeant probe whose fluorescent intensity increases upon non-covalent binding to nucleic acids. 100 µM propidium iodide was added to pulsing buffer during application of electric fields on cells grown on round coverslip. Cells were grown on a 1cm coverslip in order to be submitted to electric field with 1cm plate electrodes. Immediately afterwards, the cells were washed twice with 300 µL of PBS before being trypsinized, centrifuged and suspended in PBS, placed on ice and analyzed by flow cytometry (FACSCalibur cytometer, BD Bioscience). Finally, to discriminate between reversible and irreversible electroporation, 30 minutes after electroporation cells were removed from the incubator and were incubated for 5 minutes with 100µM propidium iodide, washed, trypsinized and analyzed by flow cytometry.

Cell viability and death measurement. A clonogenic assay was used to finely determine cell viability after application of electric field. Briefly, cells grown on round coverslip were

submitted to electric field in 100µL of pulsing buffer. After replacing it by complete culture medium, cells were incubated for 1h at 37°C to recover. After this time, cells were trypsinized, counted and 250 cells were plated into 6-well plates and placed into the incubator. 7 days after seeding, cells were washed and colored with crystal violet in order to visualize and manually count cell colonies. The percentage of dead cells through apoptosis was quantified by videomicroscopy using the IncuCyte® Caspase-3/7 Green Apoptosis Assay Reagent (Sartorius), coupled with the Nuclight Red reagent (Sartorius) to determine the total number of cells according to the manufacturer protocol. Briefly, after application of electroporation, cells were grown in culture medium containing a permeable viable DNA stain named NucLight Red Reagent (1/1000) and a caspase-3/7 recognition motif DEVD that labels cells undergoing apoptosis, i.e Caspase-3/7 green reagent (1/1000). Pictures were obtained at 10x with an IncuCyte ZOOM live cell analysis system (Sartorius), and analyzed by the MARS- associated software.

Cell synchronization. In order to assess only migration during the first 24h of the scratch wound assay, proliferation had to be inhibited. For this purpose, the overnight serum deprivation approach [32] was used as a biological way to synchronize primary dermal fibroblasts prior to scratch wound assay. Distribution of cells within cell cycle was checked by flow cytometry before the scratch experiments. Briefly, after being trypsinized and centrifuged, cells were suspended in PBS containing 5 $\mu g.mL^{-1}$ propidium iodide, 0.1% X100-Triton and 2.5% fetal bovine serum. Cells were incubated for 20 min at room temperature in the dark before flow cytometry analysis on a FACSCalibur cytometer (BD Bioscience). Cell cycle distribution was analyzed using Modfit software.

Calibrated scratch assay by videomicroscopy. In order to perform the scratch wound experiment, cells were grown at post-confluency so that when the scratch was applied, a clear and calibrated wound remained (700-800 µm wide). For this, 25 000 dermal fibroblasts were grown into ImageLock 96-well microplates (Sartorius). After 8 hours of culture, complete culture medium was removed and replaced by cell culture medium without fetal bovine serum in order to synchronize cells by serum deprivation overnight. The day of the experiment, a tool named WoundMaker (Sartorius) which is a 96-pin mechanical device designed to create homogeneous scratch wounds in cell monolayers was used. Floating scraped cells were removed and electroporation was performed in 50 µL pulsing buffer. Attention had been paid to placing electrodes parallel to the scratch wound, the cathode and anode still at the same side of the wound. After replacing pulsing buffer by 200 µL of complete cell culture medium, plates were then placed in IncuCyte ZOOM live cell analysis system (Sartorius) and pictures were taken at 10x every hour for 24h at least, and analyzed with the MARS- associated software, with the module dedicated to scratch wound assay. For galvanotaxis or electrotaxis measurements, the area colonized by fibroblasts in each wound side was quantified on Image J software (NIH) between the same picture at the moment of the scratch and 12h after. For experiments with conditioned media, 100 µL of conditioned cell culture medium were harvested 24h after electric field application on synchronized dermal fibroblast wounded monolayer and immediately placed onto a freshly synchronized dermal fibroblast wounded monolayer. Cell migration within the wound that had not been submitted to an electric field was quantified by videomicroscopy for 24h.

Cell proliferation quantification by videomicroscopy. In order to allow cell proliferation to occur over several days, 5 000 dermal fibroblasts were plated in wells of 96-well plates, a density which approximately corresponds to a confluence of 30%. After being submitted to

electric field in pulsing buffer, cells were grown in 200 µL of complete culture medium supplemented with 1/1000 Nuclight Red reagent (Sartorius) and placed within an IncuCyte ZOOM live cell analysis system (Sartorius). As a permeant DNA intercalant, it allows to clearly observe and quantify the number of nuclei over time. Pictures were taken at 10x every hour for at least 72h and analyzed with the MARS-associated software. Data obtained corresponded to the number of nuclei within the field of observation of the microscope.

Mitochondrial characterization. Mitochondrial membrane potential was assessed using MitoView 633 (Biotium) (λex = 622nm; λem = 648nm) which is a mitochondrial membrane potential-sensitive, fluorogenic dye that rapidly accumulates in mitochondria. Staining is dependent on mitochondrial membrane potential and is lost when mitochondria become depolarized [33]. Cells were labeled according to the manufacturer protocol. Briefly, cells grown in monolayer in 96-well plate were washed with PBS and then incubated for 20 minutes in the dark in a humidified atmosphere at 37°C containing 5% CO_2 with 50nM MitoView 633 in cell culture medium. Once charged with MitoView 633, cells were submitted to GET electroporation and 1h after treatment fluorescence was measured within Incucyte videomicroscope and analyzed with the MARS-associated software. Mitochondrial oxidative stress was assessed through MitoSOX Red Mitochondrial SuperOxide indicator (ThermoFisher scientific) which is a fluorogenic dye for a selective detection of superoxide in the mitochondria of living cells [34]. Once in the mitochondria, this non-fluorescent reagent is oxidized by mitochondrial superoxide when mitochondrial oxidative stress occurs to exhibit red fluorescence [35]. Cells were incubated in a 5µM of MitoSOX reagent solution and incubated 10 minutes at 37°C protected from light. MitoSOX fluorescence (λex = 510nm; λem = 580 nm) was observed by videomicroscopy on Incucyte for 12h after electroporation treatment. Pictures were analyzed with the MARS-associated software.

Genes expression analysis by PCR array. Three conditions were analyzed 4h after electric field application: control condition (n=3), ECT condition at 600V/cm (n=3) and GET condition at 200V/cm (n=2). Total RNAs of adherent dermal fibroblasts grown on 6 glass coverslips for each condition were isolated using RNeasy Micro Kit (Qiagen) strictly according to the manufacturer's instruction. The quality and quantity of isolated RNA were checked on a Nanodrop 2000 (ThermoFisher) and RNAs were then stocked at -80°C until rapid use. Reverse transcription was performed on 500ng of RNAs with the RT² HT First Strand Kit (Qiagen) according to the manufacturer's protocol. It allows an efficient first-strand cDNA synthesis and genomic DNA elimination in RNA samples. The Human Wound Healing RT² Profiler PCR Array profiles the expression of 84 key genes central to the wound healing response. For this study, we focused on growth factors sub-panel. Obtained cDNAs were directly subjected to qPCR using RT² SYBR Green qPCR Mastermix (Qiagen) and RT² Profiler PCR Array Human Wound Healing kit (Qiagen #PAHS-121Z) strictly according to the manufacturer's protocol. 96-well plate was processed into a CFX96 CFX Real-Time PCR Detection System (BioRad). Data were statistically analyzed with the associated-excel datasheet proposed by Qiagen for this gene panel. Actin, Beta-2-microglobulin, GAPDH, Hypoxanthine phosphoribosyltransferase 1 (HPRT1), ribosomal large protein P0 (RPLP0) transcripts were used for normalization. HeatMap was carried out on GraphPad Prism 8 to represent significantly up and down regulated transcripts.

Growth factor quantification by ELISA. Supernatants conditioned for 24h by dermal fibroblasts submitted to electroporation with ECT (600V/cm) and GET (200V/cm) electric parameters were stocked at -80°C until use, within a month. Vascular Endothelial Growth Factor A (VEGFA) was quantified in these supernatants using Human VEGF-A ELISA Kit

(Sigma # RAB0507, Merck KGaA, Darmstadt, Germany) according to manufacturer's protocol. Absorbance was read using a Synergy H1 (Biotek, Winooski, VT, USA) hybrid Multi-Mode Reader. Non-parametric Mann Whitney test was used to determine statistical differences between each Control, ECT, GET condition (n=5).

Statistical analyses. Data analysis was performed using GraphPad Prism 8 program (GraphPad Software, Inc., La Jolla, CA, USA) and data were expressed as mean ± SEM (standard error to the mean). Number of experiments are indicated in figure legends, where N indicates the number of independent experiments and n the total number of biological replicates. Multiple comparisons were performed using one-way analysis of variance (ANOVA) followed by Dunnett's post-test to compare every mean to the control (0V/cm) mean or two-way ANOVA followed by Bonferroni post-test to compare means within each time point. Statistics are expressed relative to the control condition (0V/cm). *$p < 0.05$, **$p < 0.01$, ***$p < 0.001$ and ****$p < 0.0001$.

Results

Distinct electric field intensities allow gradient of electropermeabilization of dermal fibroblasts. When electroporation is applied to skin tissue, the electric field distribution is heterogeneous, meaning that all the cells within the tissue do not experience the same electric field [26]. Therefore, one of the aims of this study was to submit dermal cells to distinct electric field intensities. For ECT condition, we applied a classical calibrated sequence of electric pulses (i.e 8 pulses lasting 100µs at a frequency of 1Hz) with increasing intensity, from 200V/cm to 800V/cm. For GET condition, 10 pulses lasting 5ms were applied at 1Hz frequency, with intensities ranging from 50V/cm to 300V/cm. By increasing the electric field intensity both for ECT and GET conditions, a gradual but significant increase in leakage of ATP was measured in the extracellular medium as soon as 10 minutes after electric field application (Figure 1A). To confirm that the observed ATP leakage was due to plasma membrane defaults caused by electroporation, a complementary experiment was performed by flow cytometry to quantify propidium iodide penetration within cells (Figure 1B). Both the percentage of electropermeabilized cells as well as the fluorescence intensity of these cells increased when increasing the electric field intensity in ECT and GET conditions. 100% of electropermeabilized cells were reached at 600V/cm in ECT condition and 200V/cm in GET condition. In order to be sure that the electric parameters applied induced solely a reversible and not an irreversible permeabilization, a plasma membrane resealing experiment was carried out. 30 minutes after electroporation, cells were incubated with 100µM propidium iodide and fluorescence signal was quantified by flow cytometry (Figure 1C). Less than 5% of cells were labelled with propidium iodide, regardless of the electric field intensity applied in ECT and GET condition. This means that the applied electric parameters did not induce irreversible permeabilization. The long-term cell viability after exposition to electroporation was assessed by clonogeny (Figure 1D). In the ECT condition, cell viability was not affected up to 600V/cm

but an approximately 25% loss of viability was observed at 800V/cm. The GET condition appeared to be more severe. Below 200V/cm cell viability was not affected but it fell to 50% at 300V/cm. It seems that even if irreversible electroporation was not induced by the chosen electric parameters, they still affected the long-term cell viability.

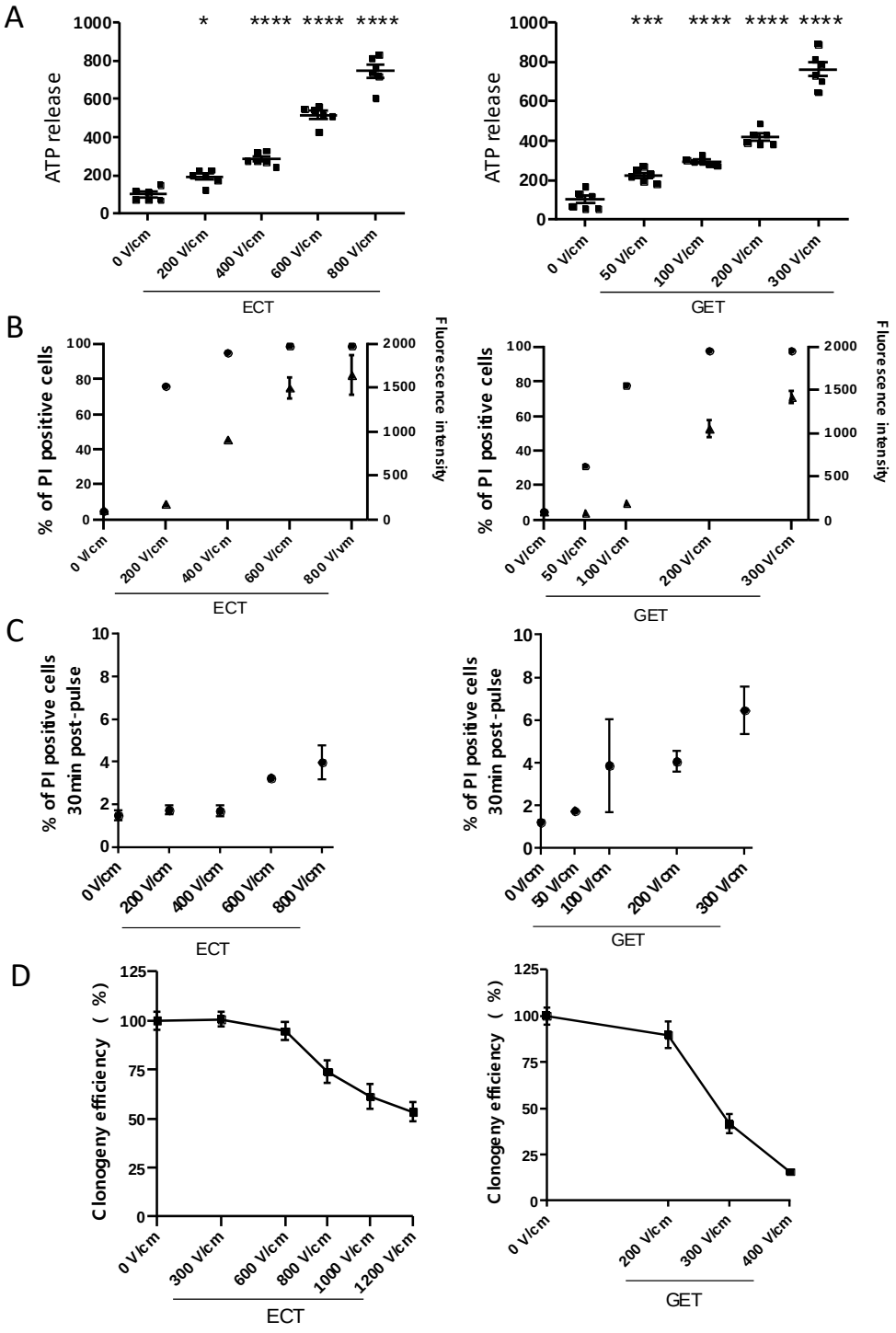

Figure 1: Determination of electric field intensity (V/cm) ensuring efficient transient cell electropermeabilization without affecting cell viability. A. Quantification of ATP release 10 min after the application of ECT and GET electrical parameters, expressed as % of control. N=2; n=6. Statistical analysis by One-way ANOVA *=p<.05; ***=p<.001; ****=p<.0001. B. Monitoring of cell electropermeabilization immediately after the application of ECT and GET electrical parameters. Left axis: % of propidium iodide (PI) positive cells (dot ●); Right axis: fluorescence intensity (triangle ▲). n=3. C. Monitoring of plasma membrane resealing 30min after the application of ECT and GET electrical parameters. n=3. D. Long term cell viability after the application of ECT and GET electrical parameters, N=3; n=9. Data are represented as the mean value ± SEM. ECT: electrochemotherapy; GET: gene electrotransfer.

Migratory properties of human primary dermal fibroblasts are not statistically affected by the application of ECT and GET electric parameters. In scratch wound assay, cells migrate and proliferate to fill the gap, thus, it is classically desired to suppress proliferation component in order to measure only cell migration during the first 24h [36]. The *in vitro* synchronization of dermal fibroblasts was achieved using overnight serum deprivation, a non-pharmaceutical method. Cellular DNA content was determined by staining cells with propidium iodide and measuring fluorescence by flow cytometry. The proportion of cells in the different phases of cell cycle were calculated depending on the cell's DNA content (n): G1 (2n), S (between 2n and 4n), and G2 (4n). As shown in Fig 2A, primary dermal fibroblasts were highly responsive to this method since approximately 90% of the cells were synchronized in the growing phase G1 using this method. With its scratch wound module, the IncuCyte ZOOM live cell analysis system allows to properly measure cell migration in calibrated scratch wound assay. Wound confluence was determined each hour after electric field application for 24h using image processing with masks (Figure 2B and Movie 1).,. Movie 2 showed that wound closure by dermal fibroblasts was a highly dynamic process. As previously explained, wound closure was analyzed only for the first 24h after application of electric field on synchronized cells in order to take into account solely the migration component. The absence of cell division events (rounding cell before splitting in two round cells) on the movie during the first 24h confirmed this assumption. After 24h, cell confluence within the wound was approximately 40%, whatever the ECT or GET condition (Figure 2C). It is noteworthy that cell migration occurred

immediately after wounding, and continued regularly over hours, with or without application of ECT or GET electric parameters. No statistical difference was observed on the time course of the migration depending on the electric parameters applied, but a linear regression was performed to obtain the speed of migration of each condition during the first 12h (Figure 2D). Even if no statistical difference was observed whatever the conditions were, taking account standard error to the mean, ECT 600V/cm and 800V/cm as well as GET 50V/cm and 100V/cm conditions presented a slight increase in speed of migration. Finally, the wound confluence 24h post-electric field application was finely analyzed (Figure 2E). GET conditions at 50V/cm and 100V/cm seemed to improve dermal fibroblast migration and thus wound healing, but despite numerous repetitions of the experiments and biological replicates (until 30) no statistical difference was observed, so it remained a trend.

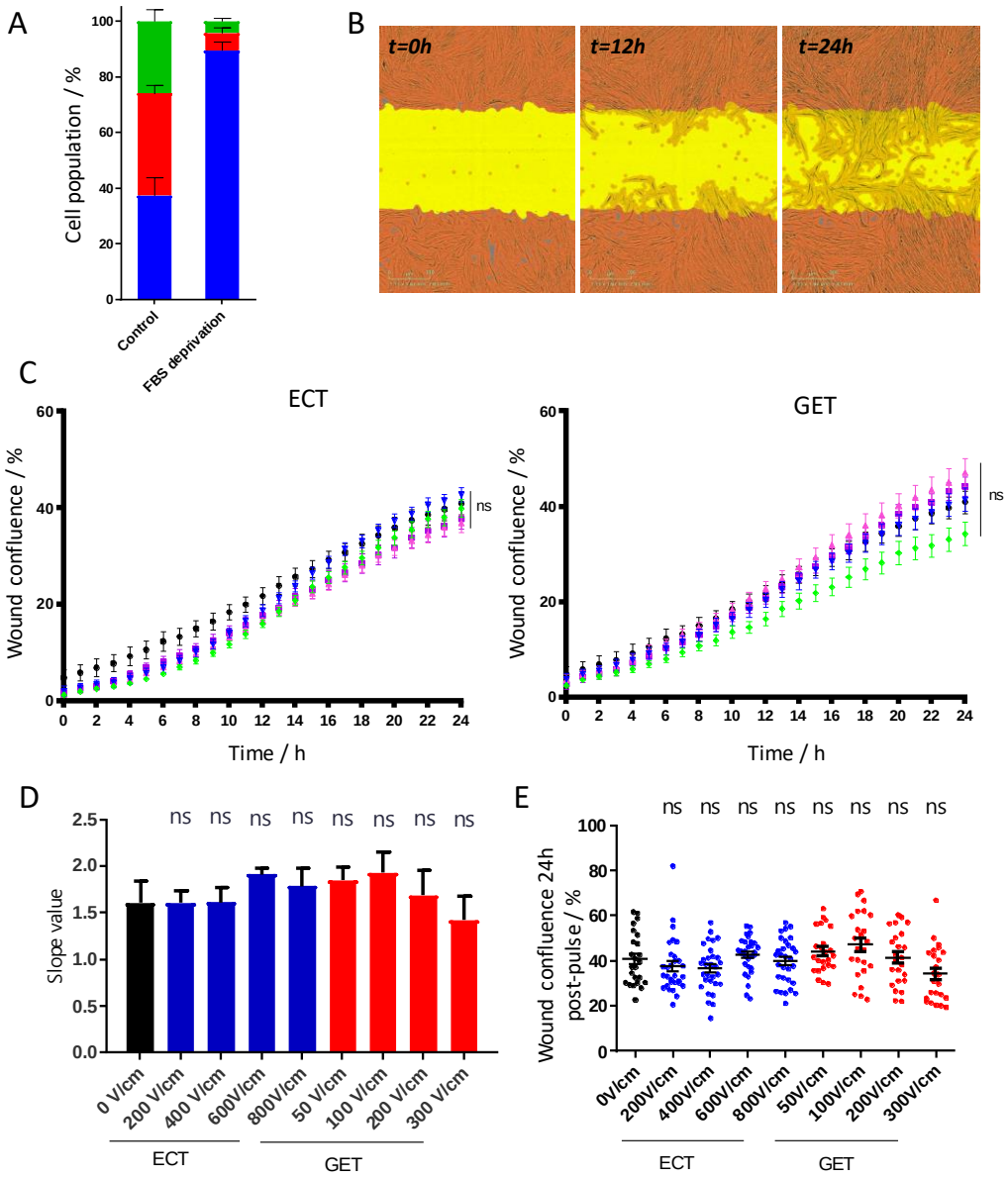

Figure 2: ECT and GET electrical parameters did not affect dermal fibroblast migration properties in scratch wound assay. A. Cell cycle synchronization after overnight fetal bovine serum (FBS) deprivation. Phases G1 in blue, S in red and G2 in green. N=3; n=8. B. Image processing with masks to quantify dermal fibroblasts migration in scratch wound assay.C. Time course of cell migration after the application of ECT (x8 pulses lasting 100µs, 1Hz frequency, at 0V/cm (●), 200V/cm (■), 400 V/cm (▲), 600V/cm (▼), 800V/cm (♦)) and GET (x10 pulses lasting 5ms, 1Hz frequency, at 0V/cm (●), 50V/cm (■), 100 V/cm (▲), 200V/cm (▼), 300V/cm (♦)) electrical parameters on synchronized fibroblasts wounded monolayer. N=5; n= 30 Statistical analyses by Two-Way ANOVA. D. Slope values calculated by linear regression during the first 24h. N=3, n=9. E. Wound confluence (%) 24h after the application of ECT and GET electrical parameters. N=5; n= 30. Statistical analysis by One-Way ANOVA. Data are represented as the mean value ± SEM. ECT: electrochemotherapy; GET: gene electrotransfer.

No galvanotaxis of dermal fibroblasts is induced by ECT and GET electric parameters.

The external electric field is a major physical cue of the microenvironment that guides

directional migration. This phenomenon is called galvanotaxis or electrotaxis. Since the plate electrodes were systemically placed parallel to the wound, anode on the top and cathode on the bottom, we were able to determine if fibroblasts at the margin of the wound displayed preferential directed migration (Figure 3). No statistical differences were observed, meaning that dermal fibroblasts migrated equally toward the cathode or anode side.

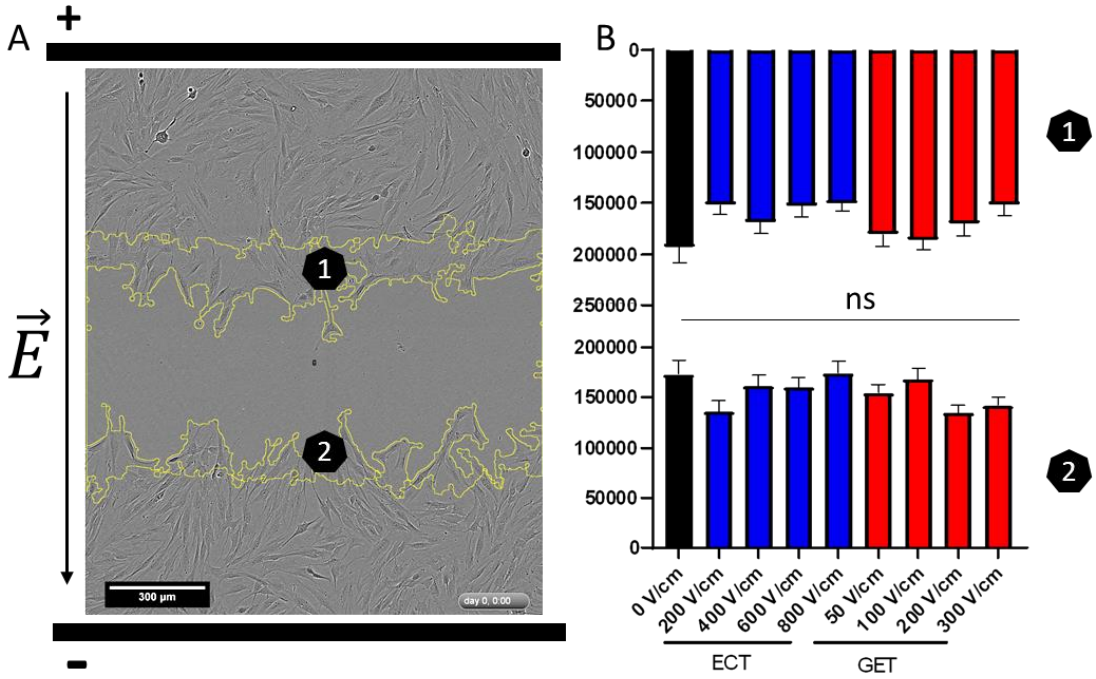

Figure 3: No electrotaxis was observed in dermal fibroblasts when submitted to ECT and GET electrical parameters. A. Schematic representation of electrodes position at the wound site. Yellow line delimits cell-occupied area in the anode panel (1) and cathode panel (2). B. Cell-occupied area (μm^2) either upper panel of the wound (1) or lower panel of the wound (2) 12h after electric field application. Data are represented as the mean ± SEM. Statistical analysis by One-Way Anova. N=3; n=18.

High GET electric parameters drastically reduce the number of dermal fibroblast . Evolution of cell number over 72h after ECT and GET application was followed by videomicroscopy (Movie 3) through automatically counting fluorescently labelled nuclei within the microscope field (Figure 4A). ECT electric parameters did not lead to statistical difference between the control condition and the distinct electric field intensity applied, even if 200V/cm

and 400V/cm growth curves tended to be higher than the control one (0V/cm) (Figure 4B). For GET conditions, three distinct behaviors had to be differentiated. Cells submitted to electric fields of 50 and 100V/cm behaved similarly to the control condition. On the other hand, from 200V/cm, the number of nuclei decreased with a significant delay, and this phenomenon was increased for higher electric field intensity (300V/cm). This observation was confirmed by analyzing the number of nuclei within the microscope field 70h after electric field application (Figure 4C). The delay in cell growth can be explained either by a stop in cell proliferation or by a dynamic equilibrium between dying cells and proliferative cells, as we observed by clonogenic assay that GET at 300V/cm altered long-term cell viability by 60% (Fig 1D).

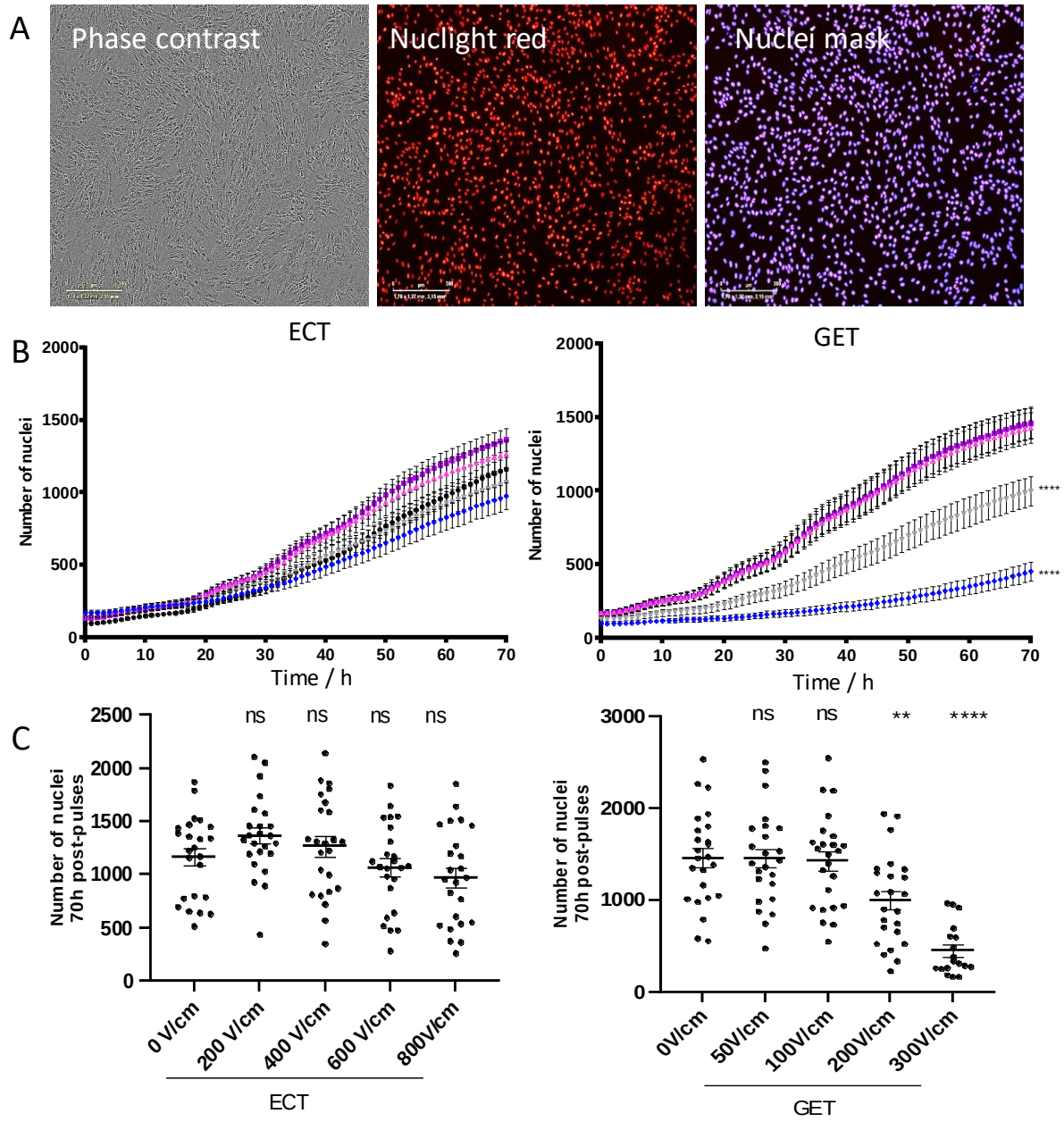

Figure 4: ECT electrical parameters did not affect dermal fibroblast proliferation while some GET parameters reduced cell number. A. Image processing with masks to quantify dermal fibroblasts proliferation. B. Dermal fibroblasts proliferation after application of ECT (x8 pulses lasting 100µs, 1Hz frequency, at 0V/cm (●), 200V/cm (■), 400 V/cm (▲), 600V/cm (▼), 800V/cm (♦)) and GET (x10 pulses lasting 5ms, 1Hz frequency, at 0V/cm (●), 50V/cm (■), 100 V/cm (▲), 200V/cm (▼), 300V/cm (♦)) electrical parameters. Statistical analysis by Two-Way ANOVA ****=p<.0001 C. Number of nuclei 70h after the application of ECT and GET electrical parameters. N=6; n=24. Statistical analysis by One-Way ANOVA *=p<.05; **=p<.01; ****=p<.0001. Data are represented as the mean value ± SEM.

High GET electric parameters induce dermal fibroblast apoptosis through mitochondrial stress. Only certain electric field intensities in GET conditions have shown anti-proliferative results on cell monolayers, thus we decided to focus on GET electric parameters for apoptosis and mitochondrial stress analysis. In order to explain the delay observed in cell growth after GET electric parameter application, apoptosis was investigated 24h after electroporation (figure 5A). The percentage of cells dying by apoptosis increased when the electric field intensity increased. At 200V/cm approximately 10% of the cells displayed activated caspases3/7 and this percentage reached 30% at 300V/cm 24h after electric field application. This 30% of apoptotic cells in 300V/cm condition differed from the one observed by clonogenic assay (loss of 60% of long-term cell viability, Fig 1D), meaning that other cell death mechanisms could be involved, such as necrosis. We previously showed that mitochondria ultrastructure was rapidly altered after cells were submitted to electroporation [37]. Consequently, we focused subsequent experiments on mitochondrial characterization. A MitoView fluorescent probe was used to follow the mitochondrial membrane potential after application of GET electric parameters (Figure 5B). The fluorescent staining depends on the mitochondrial membrane potential and is lost when mitochondria become depolarized [33]. A significant loss of staining was observed on live cells 1h after GET electric field application at 300V/cm, meaning that mitochondria underwent depolarization, which could lead to initiation of cell death processes, especially apoptosis [38]. We used videomicroscopy to follow mitochondrial oxidative stress in live cells after GET application using the MitoSOX reagent (Figure 5C). This probe selectively targets mitochondria and becomes highly fluorescent after oxidation specifically by mitochondrial superoxide [34]. No immediate mitochondrial oxidative stress was observed after GET electric parameters application, but a delayed effect was observed for 200V/cm and 300V/cm intensity from 4h after pulses, and became statistically significant 7h after pulses. This means that at

200V/cm and even more at 300V/cm, oxidant mitochondrial stress was generated as soon as 4h after electroporation, through generation of mitochondrial superoxide.

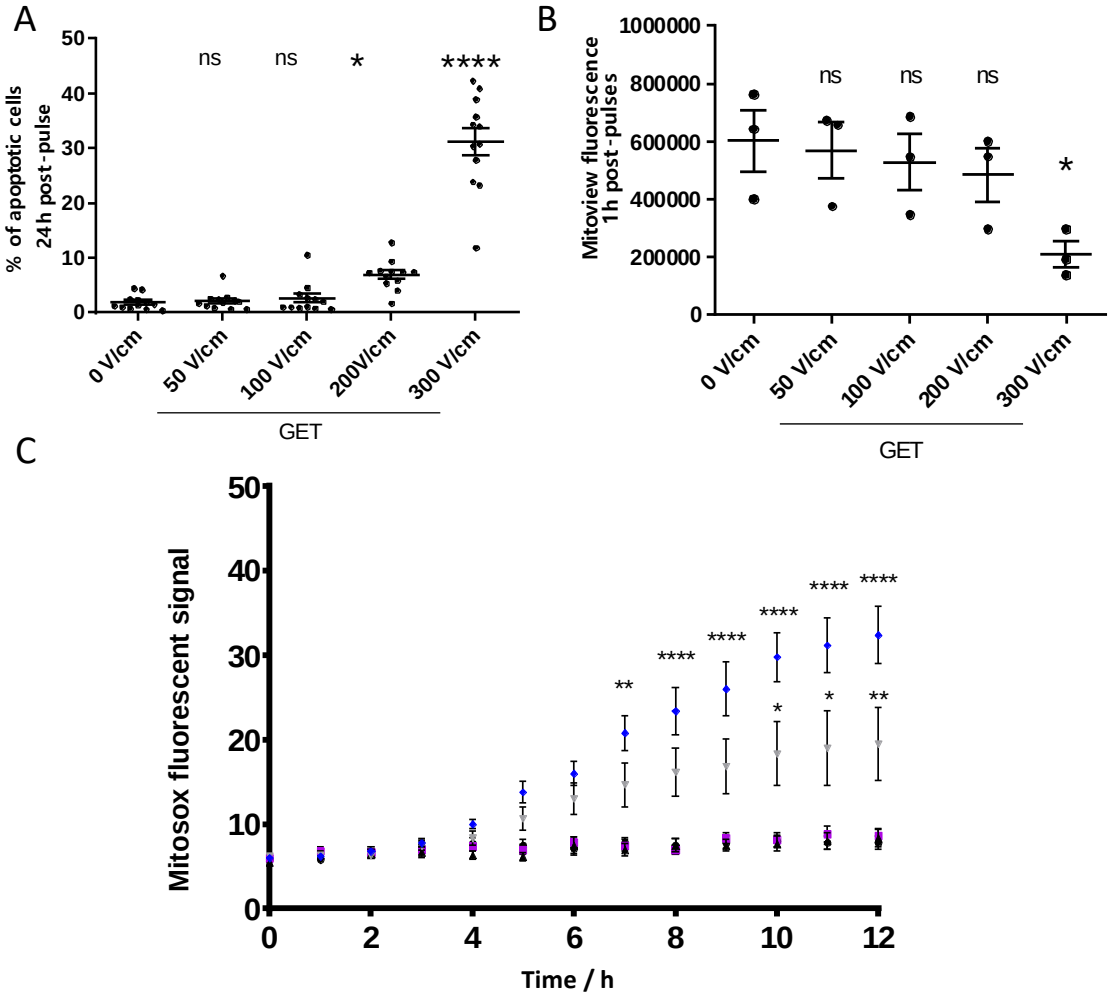

Figure 5: Some GET electrical parameters induced apoptosis through mitochondrial stress. A. Percentage of apoptotic cells. N=2; n=12. Statistical analysis by One-way and Two-way ANOVA *=p<.05; ****=p<.0001 B. Quantification of mitochondrial membrane potential loss 1h after electric field application. N=1; n=3. Statistical analysis by One-way ANOVA *=p<.05 C. Fluorescent detection of generation of mitochondrial superoxide anion $O_2^{\cdot-}$ after application of GET (x10 pulses lasting 5ms, 1Hz frequency, at 0V/cm (●), 50V/cm (■), 100 V/cm (▲), 200V/cm (▼), 300V/cm (♦)) electrical parameters. N=2; n=12. Data are represented as the mean value ± SEM. Statistical analysis by Two-way ANOVA *=p<.05; **=p<.01; ****=p<.0001.

Unexposed fibroblast migration properties were stimulated by 24h-conditioned media. In order to assess the indirect effects of electric field application on the migration properties of dermal fibroblasts, scratch wound assays with cells cultured in conditioned media were performed (Figure 6). In this condition, analyzed dermal fibroblasts were never submitted to electric field, but only exposed to cell culture medium conditioned for 24h by dermal fibroblasts

that had themselves been exposed to different conditions of ECT and GET. Statistical analyses on a large number of replicates indicated that over the first 24h the conditioned media of GET 200V/cm condition improved wound closure compared to control condition. A trend emerged from 10h, which became statistically significant at 18h and then increased over the last 6 hours of the experiment. However, these analyses did not reveal statistical differences for the other GET conditions nor for the ECT conditions (figure 6A). Cell confluence within wound area after 24h of culture in conditioned media indicated a global trend for all conditioned-media conditions to stimulate cell migration (Figure 6B). However, only the conditioned media of GET 200V/cm condition statistically improved the wound healing in the scratch wound assay. It has to be underlined that the electric parameters applied in this condition were the ones leading to moderate apoptosis. We thus hypothesized that dermal fibroblasts exposed to pulsed electric fields and undergoing light apoptosis secreted several factors stimulating unexposed fibroblasts to migrate in the wound area.

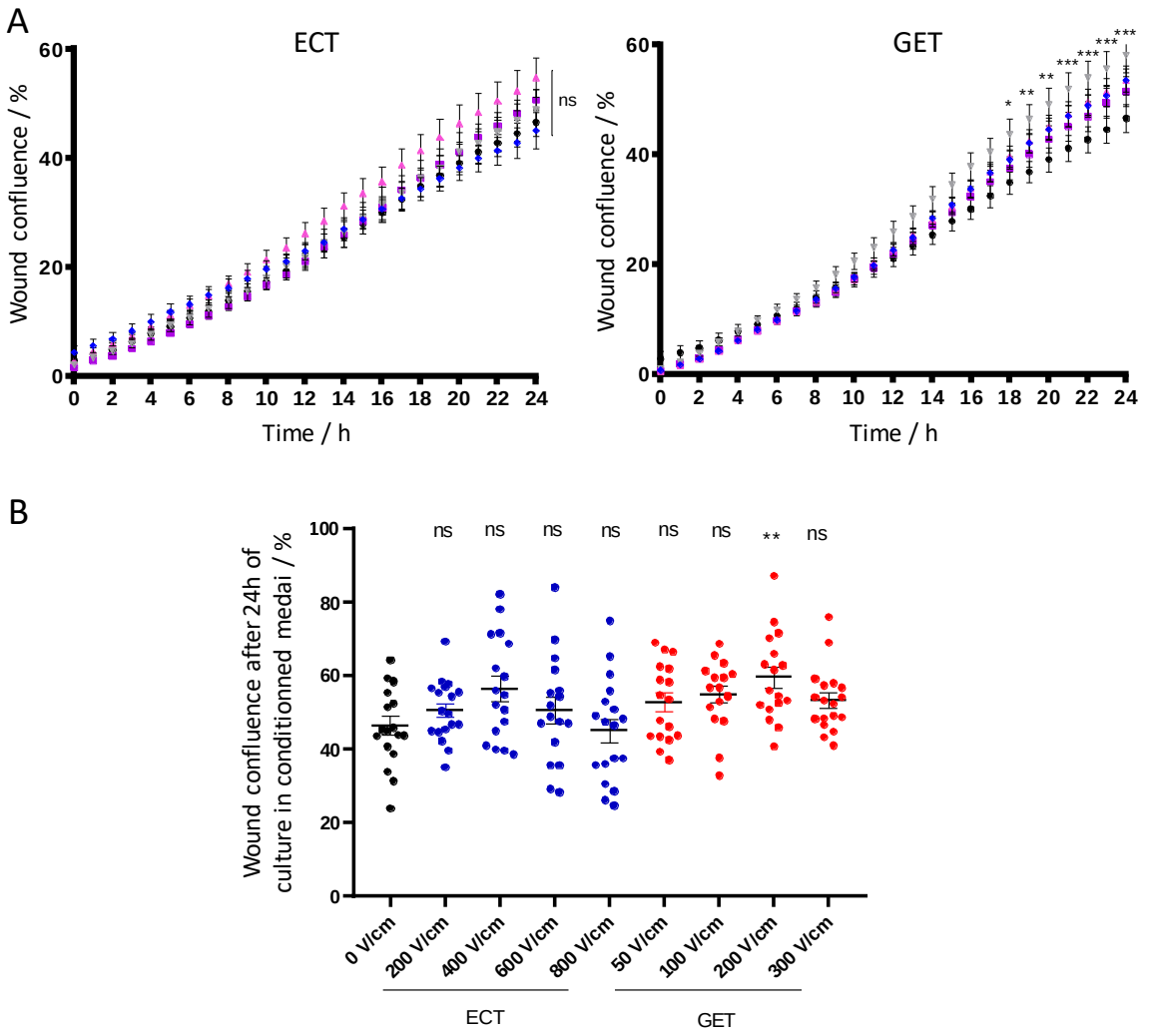

Figure 6: Conditioned media from electroporated-fibroblasts stimulated the migration of unexposed fibroblasts. A. Migration of dermal fibroblasts cultured in 24h ECT-(x8 pulses lasting 100µs, 1Hz frequency, at 0V/cm (●), 200V/cm (■), 400 V/cm (▲), 600V/cm (▼), 800V/cm (♦)) and and GET-(x10 pulses lasting 5ms, 1Hz frequency, at 0V/cm (●), 50V/cm (■), 100 V/cm (▲), 200V/cm (▼), 300V/cm (♦)) conditioned cell culture media. N=3; n= 18. Only the 200V/cm condition showed statistical difference with the control condition (0V/cm). Statistical analysis by Two Way ANOVA *=p<.05; **=p<.01; ***=p<.001 B. Wound confluence after 24h of culture in 24h ECT- or GET-conditioned media. N=3; n=18. Data are represented as the mean value ± SEM. Statistical analysis by One-way ANOVA **=p<.01.

ECT and GET electric parameters strongly modulate growth factor transcripts. In order to understand the above results, a commercially available qPCR array dedicated to wound healing was performed 4h after exposure to ECT and GET electric parameters. This analysis revealed significant variations in the number of growth factor transcripts (Figure 7A).

Overexpressed genes (in red in the figure) in both conditions include Connective Tissue Growth Factor (CTGF), Vascular Endothelial Growth Factor A (VEGFA), Platelet Derived Growth Factor Subunit A (PDGFA), and Transforming Growth Factor Alpha (TGFα) with 1.2- to 3.6-fold increases compared to non-electroporated controls. Several growth factors were also under-expressed (in green in the figure) 4h after exposure to ECT and GET electric parameters including TGF-β1 a well-known protagonist in dermal fibrosis. For GET parameters we also noted specific over-expressions of immunity-related factors like Colony stimulating factor 3 (CSF3), as well as angiogenic factors like Epidermal growth factor (EGF). This experiment confirmed that the expression of several growth factors transcripts was rapidly and strongly modulated after cell electroporation. To confirm that this modulation of growth factors transcripts was also observed at protein level, we quantified one using ELISA in cell culture medium 24h after electroporation of dermal fibroblasts (Figure 7B). We focused on Vascular Endothelial Growth Factor A (VEGFA) because it was the more over-expressed at the RNA level (2.4 times in ECT and 3.3 times in GET conditions). More VEGFA protein was indeed found in cell culture supernatant 24h after electroporation both in ECT condition (even if not statistically significant) and in GET condition (statistically significant). We thus confirmed at protein level that electroporation, especially GET condition, increases the expression of VEGFA growth factor, as observed at transcriptional level.

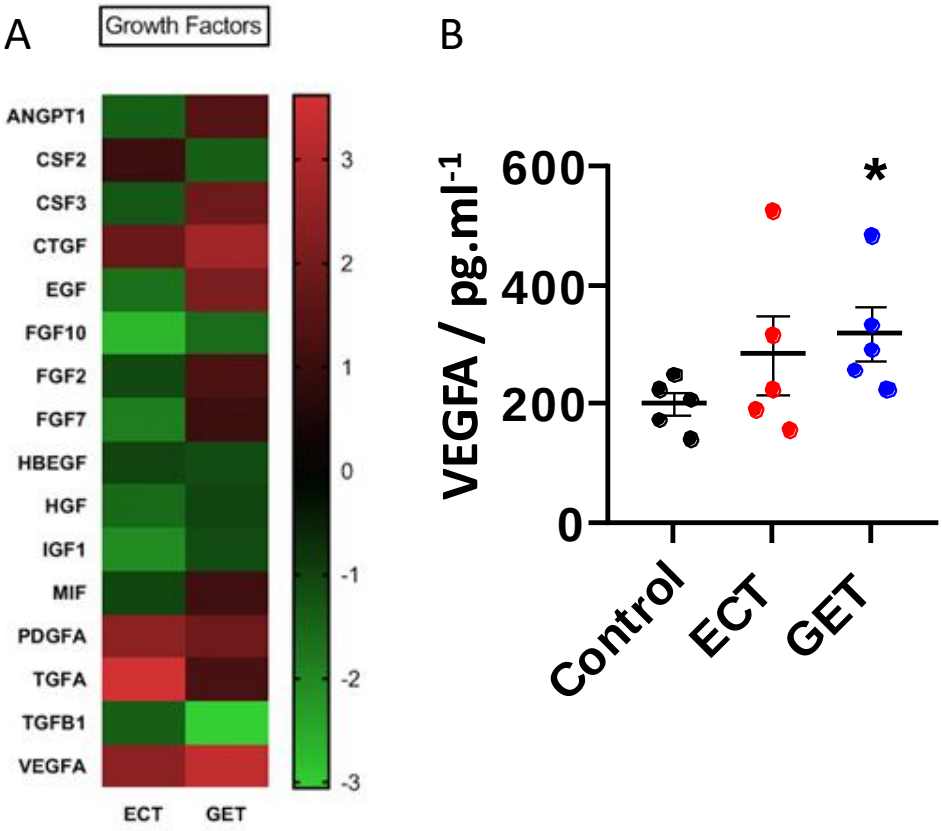

Figure 7: Gene expression analysis of growth factor related genes in dermal fibroblasts 4h after exposure to ECT and GET electric parameters. A. Gene expression was quantified by RT-qPCR array. Fold changes are expressed compared to the control condition. Control and ECT condition (600V/cm) n=3, GET condition (200V/cm) n=2. Angiopoietin 1 (ANGPT1); Colony stimulating factor 2,3 (CSF2,3); Connective Tissue Growth Factor (CTGF); Epidermal growth factor (EGF); Fibroblast growth factor 2,7,10 (FGF2,7,10); Heparin binding EGF like growth factor (HBEGF); Hepatocyte growth factor (HGF); Insulin like growth factor 1 (IGF1); Macrophage migration inhibitory factor (MIF); Platelet Derived Growth Factor Subunit A (PDGFA); Transforming Growth Factor Alpha (TGFα); Transforming Growth Factor Beta 1 (TGF-β1); Vascular Endothelial Growth Factor A (VEGFA). B. VEGFA protein expression quantified by ELISA in cell culture medium 24h after dermal fibroblasts electroporation with ECT (600V/cm) and GET (200V/cm) electric parameters N=1, n=5. Statistical analysis by Mann Whitney test *=p<.05.

Discussion

The existence of a physiological transepithelial electric potential within the skin makes skin cells a good target for testing modulation of behavior through electroporation application. Endogenous electric fields are important to guide cell migration and often predominate over chemical or topographic signals [39]. Directional migration along an electric field guiding cue has already been shown in fibroblast cells [24,40,41]. Human dermal fibroblasts submitted to an electric field of 50–200 mV mm^{-1} under direct current took more than 1 hour to exhibit measureable directional migration toward the anode [24,41]. Zhao *et al.* have identified Phosphatidyl-Inositol 3 Kinase (PI(3)K) and Phosphatase and tensin homolog (PTEN) as essential genes controlling the electrotaxis [24]. Indeed, the electric field directs cell migration by acting as the primary directional signal, triggering Tyrosine-protein Kinase Src and Inositol-phospholipid signalling pathways. The role of Phosphatidyl-Inositol 3 Kinase in electro-induced migration was confirmed by Guo and colleagues in 2010 [41]. Another suggested mechanism is the asymmetric redistribution of EGFR membrane receptors on the cell surface [42–44]. Nevertheless, these studies mainly applied long exposure direct currents, whereas in this study we used a pulsed electric field. The difference in the nature and intensity of the applied electric fields could explain the absence of significate results in migration and galvanotaxis experiments with electroporation.

High-voltage pulsed galvanic stimulation has been shown to have a proliferative effect on human foetal lung fibroblasts IMR-90 and to stimulate protein synthesis [45]. This study indicated an increase in protein synthesis rates 2h post stimulation and in DNA synthesis between 2 and 24h post stimulation. The maximum increases in protein and DNA synthesis occurred with electric parameters of 100 pulses/seconds and 50 and 75 V/cm respectively. In this study, electrical parameters were applied for at least 20 min, far from the pulsed electric

field applied in electroporation. Thus, the involved molecular mechanisms may differ and explain the absence of proliferation after ECT and GET application.

Reactive oxygen species (ROS) play a major role in wound healing response [46,47]. Interestingly, it has previously been shown that electroporation generates ROS such as H_2O_2 [48,49]. Studies on lipid peroxidation in cell membranes after electroporation have been reported [48–50]. Lipids peroxidation and ROS concentration increase with electric field intensity, pulse duration and number of pulses and is correlated to membrane electropermeabilization and to cell death when the amount of cellular damage is too high [51]. ROS can be involved in the recruitment of immune cells [52,53], in the regulation of angiogenesis processes [46,54] and they present bacteriostatic effects at wound sites [55]. However, high production of ROS may lead to impaired wound repair [56]. In these conditions ROS will give rise to the secretion of pro-inflammatory cytokines, of metalloproteases, and can impair the function of dermal fibroblasts and keratinocytes [57]. Moreover, ROS are generally associated with skin ageing, fibroblast senescence and autophagy [58]. In our experimental conditions, electroporation of dermal fibroblasts with the highest electric field intensities in GET condition (200V/cm and 300V/cm) blocked migration process and induced cell death. These results are in agreement with those reported in the literature showing the deleterious effects of H_2O_2 on dermal fibroblasts [59,60].

We demonstrated that modulating the intensity of the electric fields led to a gradient of cell electropermeabilization. We can hypothesize that cell responses to these different plasma membrane defaults will be different. Indeed, apoptotic cell death induction was observed for the most stressful GET electrical parameters (i.e 200V/cm and 300V/cm). The secretome in a culture medium that was conditioned in these electric conditions improved the ability of unexposed dermal fibroblasts to migrate. We can theorize that this bystander effect can occur *in vivo*, where dying cell would secrete specific factors modifying surrounding cells behavior.

It was previously demonstrated in electroporation that electric field alone induced the externalization of calreticulin [61] while calreticulin is usually an endoplasmic reticulum-resident protein. When externalized, it becomes a danger-associated molecular pattern molecule (DAMP) associated with the induction of immunogenic cell death [62]. Interestingly, studies showed that calreticulin externalization played a significant role in cutaneous wound healing by stimulating dermal fibroblast and keratinocyte proliferation, migration, and differentiation [63]. Several studies have already shown that nucleotides released from damaged tissues, such as extracellular ATP or purines and pyrimidines released following cell death and DNA fragmentation, regulate many important functions of skin cells (proliferation, migration, contraction) and can promote wound healing [64].

Further experiments would be needed to finely describe what kind of factors are secreted or released by the dying cells. We obtained encouraging results on the modulation of a number of growth factors transcripts by electroporation. One of them, VEGFA, was quantified at protein level by ELISA. In our experimental condition, we demonstrated that electroporated dermal fibroblasts released in cell culture a significant amount of VEGFA. However, comprehensive analyses of both growth factors and cytokines secreted as a result of electroporation should be exhaustively conducted at protein level (ELISA, proteomic, secretome profiling) and functional tests are essential to conclude in our experimental conditions. Interestingly, cues can be found in the literature to enrich the reflection on this bystander effect. Some authors used pulsed electric field to activate platelets. They showed that electroporation stimulates the release of growth factors such as PDGF-AA, TGF-β1 or EGF, contained in granules within the cells [65]. A modulation of pulsed electric field parameters led to a differential growth factors release [66].

Bystander effect induced by electroporation was previously investigated in the context of melanoma tumor cells [67]. In this context, a negative bystander effect leading to death of cells cultivated in conditioned medium was observed and could be due to release of microvesicles

(<500nm). Interestingly, the bystander effect and microvesicles amounts depended on electric parameters (pulse amplitude and repetition frequency), confirming that in tissue cell response will be different depending on electric field distribution. Since electroporation affects plasma membrane integrity, it would be of utmost importance to characterize well and screen the induced extracellular vesicles, which can contain proteins, RNA molecules and other agents, able to influence signaling pathways in distant cells.

In this line of thought on communication between cells, co-culture of cells would be a complementary approach to the one adopted in this study. In our case, a co-culture of dermal cells (primary fibroblasts) with epidermal cells (primary keratinocytes) would be relevant. To go forward, *in vitro* cell culture models should switch from 2D to 3D tissue models. Even if 2D cell cultures are easier to manage, it is now widely accepted that 3D models better mimic *in vivo* situations [68]. In skin context, some *in vitro* 3D tissue models such as spheroids [69], dermal cell sheets [29,70] or recellularized human skin biopsy [71] have been developed and used in electroporation study. The next step would be to use them for fundamental studies to better understand links between electroporation and wound healing.

Author Contributions. conceptualization, L.G.; investigation and formal analyses, S.G., A.D., L.G.; writing-original draft preparation, S.G. and L.G.; writing-review and editing, S.G., AF.M., P.V., MP.R., L.G.; scientific discussion, S.G., A.D., AF.M., P.V., MP.R., L.G.; supervision, L.G.; funding acquisition, MP.R., L.G.

Funding. This research was funded by the French Agence Nationale de la recherche, ANR-17-CE19-0013-01 and NUMEP Plan Cancer PC201615 grant.

Acknowledgments. We would like to thank the Imaging and flow cytometry Core Facility TRI-IPBS. We would like to warmly thank Dr Ahmed Amine Khamlichi and Audrey Dauba for their help in RT-qPCR array experiments. We kindly acknowledge Simon Harrisson, a native English scientist, for his careful proofreading of this manuscript.

Conflicts of Interest. The authors declare no conflict of interest. The funders had no role in the design of the study; in the collection, analyses, or interpretation of data; in the writing of the manuscript, or in the decision to publish the results.

References

[1] E. Neumann, K. Rosenheck, Permeability changes induced by electric impulses in vesicular membranes, J. Membr. Biol. 10 (1972) 279–290.

[2] J. Teissie, M. Golzio, M.P. Rols, Mechanisms of cell membrane electropermeabilization: a minireview of our present (lack of?) knowledge, Biochim. Biophys. Acta BBA-Gen. Subj. 1724 (2005) 270–280.

[3] M.L. Yarmush, A. Golberg, G. Serša, T. Kotnik, D. Miklavčič, Electroporation-Based Technologies for Medicine: Principles, Applications, and Challenges, Annu. Rev. Biomed. Eng. 16 (2014) 295–320. https://doi.org/10.1146/annurev-bioeng-071813-104622.

[4] L.G. Campana, I. Edhemovic, D. Soden, A.M. Perrone, M. Scarpa, L. Campanacci, M. Cemazar, S. Valpione, D. Miklavčič, S. Mocellin, E. Sieni, G. Sersa, Electrochemotherapy – Emerging applications technical advances, new indications, combined approaches, and multi-institutional collaboration, Eur. J. Surg. Oncol. 45 (2019) 92–102. https://doi.org/10.1016/j.ejso.2018.11.023.

[5] E.P. Spugnini, A. Baldi, Electrochemotherapy in Veterinary Oncology, Vet. Clin. North Am. Small Anim. Pract. 49 (2019) 967–979. https://doi.org/10.1016/j.cvsm.2019.04.006.

[6] J. Gehl, G. Sersa, L.W. Matthiessen, T. Muir, D. Soden, A. Occhini, P. Quaglino, P. Curatolo, L.G. Campana, C. Kunte, A.J.P. Clover, G. Bertino, V. Farricha, J. Odili, K. Dahlstrom, M. Benazzo, L.M. Mir, Updated standard operating procedures for electrochemotherapy of cutaneous tumours and skin metastases, Acta Oncol. 57 (2018) 874–882. https://doi.org/10.1080/0284186X.2018.1454602.

[7] E. Kis, E. Baltás, Á. Kinyó, E. Varga, N. Nagy, R. Gyulai, L. Kemény, J. Oláh, Successful Treatment of Multiple Basaliomas with Bleomycin-based Electrochemotherapy: A Case Series of Three Patients with Gorlin-Goltz Syndrome, Acta Derm Venereol. 92 (2012) 648–51. https://doi.org/10.2340/00015555-1361.

[8] L.F. Glass, M. Jaroszeski, R. Gilbert, D.S. Reintgen, R. Heller, Intralesional bleomycin-mediated electrochemotherapy in 20 patients with basal cell carcinoma, J. Am. Acad. Dermatol. 37 (1997) 596–599. https://doi.org/10.1016/S0190-9622(97)70178-6.

[9] M. Marty, G. Sersa, J.R. Garbay, J. Gehl, C.G. Collins, M. Snoj, V. Billard, P.F. Geertsen, J.O. Larkin, D. Miklavcic, I. Pavlovic, S.M. Paulin-Kosir, M. Cemazar, N. Morsli, D.M. Soden, Z. Rudolf, C.

Robert, G.C. O'Sullivan, L.M. Mir, Electrochemotherapy – An easy, highly effective and safe treatment of cutaneous and subcutaneous metastases: Results of ESOPE (European Standard Operating Procedures of Electrochemotherapy) study, Eur. J. Cancer Suppl. 4 (2006) 3–13. https://doi.org/10.1016/j.ejcsup.2006.08.002.
[10] L.G. Campana, S. Mocellin, M. Basso, O. Puccetti, G.L. De Salvo, V. Chiarion-Sileni, A. Vecchiato, L. Corti, C.R. Rossi, D. Nitti, Bleomycin-Based Electrochemotherapy: Clinical Outcome from a Single Institution's Experience with 52 Patients, Ann. Surg. Oncol. 16 (2009) 191–199. https://doi.org/10.1245/s10434-008-0204-8.
[11] L. Gibot, M.-P. Rols, Gene transfer by pulsed electric field is highly promising in cutaneous wound healing, Expert Opin. Biol. Ther. 16 (2016) 67–77. https://doi.org/10.1517/14712598.2016.1098615.
[12] M.P. Lin, G.P. Marti, R. Dieb, J. Wang, M. Ferguson, R. Qaiser, P. Bonde, M.D. Duncan, J.W. Harmon, Delivery of plasmid DNA expression vector for keratinocyte growth factor-1 using electroporation to improve cutaneous wound healing in a septic rat model, Wound Repair Regen. 14 (2006) 618–624.
[13] G. Basu, H. Downey, S. Guo, A. Israel, A. Asmar, B. Hargrave, R. Heller, Prevention of distal flap necrosis in a rat random skin flap model by gene electrotransfer delivering VEGF165 plasmid, J. Gene Med. 16 (2014) 55–65.
[14] B. Ferraro, Y.L. Cruz, M. Baldwin, D. Coppola, R. Heller, Increased perfusion and angiogenesis in a hindlimb ischemia model with plasmid FGF-2 delivered by noninvasive electroporation, Gene Ther. 17 (2010) 763.
[15] L. Steinstraesser, M.C. Lam, F. Jacobsen, P.E. Porporato, K.K. Chereddy, M. Becerikli, I. Stricker, R.E. Hancock, M. Lehnhardt, P. Sonveaux, Skin electroporation of a plasmid encoding hCAP-18/LL-37 host defense peptide promotes wound healing, Mol. Ther. 22 (2014) 734–742.
[16] G. Marti, M. Ferguson, J. Wang, C. Byrnes, R. Dieb, R. Qaiser, P. Bonde, M.D. Duncan, J.W. Harmon, Electroporative transfection with KGF-1 DNA improves wound healing in a diabetic mouse model, Gene Ther. 11 (2004) 1780–1785. https://doi.org/10.1038/sj.gt.3302383.
[17] P.-Y. Lee, S. Chesnoy, L. Huang, Electroporatic Delivery of TGF-β1 Gene Works Synergistically with Electric Therapy to Enhance Diabetic Wound Healing in db/db Mice, J. Invest. Dermatol. 123 (2004) 791–798. https://doi.org/10.1111/j.0022-202X.2004.23309.x.
[18] S. Ud-Din, A. Bayat, Electrical stimulation and cutaneous wound healing: a review of clinical evidence, in: Healthcare, Multidisciplinary Digital Publishing Institute, 2014: pp. 445–467.
[19] I.S. Foulds, A.T. Barker, Human skin battery potentials and their possible role in wound healing, Br. J. Dermatol. (1983). https://onlinelibrary.wiley.com/doi/abs/10.1111/j.1365-2133.1983.tb07673.x (accessed August 19, 2019).
[20] I.S. Foulds, A.T. Barker, Human skin battery potentials and their possible role in wound healing, Br. J. Dermatol. 109 (1983) 515–522. https://doi.org/10.1111/j.1365-2133.1983.tb07673.x.
[21] R. Nuccitelli, Endogenous ionic currents and DC electric fields in multicellular animal tissues, Bioelectromagnetics. 13 (1992) 147–157. https://doi.org/10.1002/bem.2250130714.
[22] A.T. Barker, L.F. Jaffe, J.W. Vanable, The glabrous epidermis of cavies contains a powerful battery, Am. J. Physiol.-Regul. Integr. Comp. Physiol. 242 (1982) R358–R366. https://doi.org/10.1152/ajpregu.1982.242.3.R358.
[23] B. Reid, M. Zhao, The electrical response to injury: molecular mechanisms and wound healing, Adv. Wound Care. 3 (2014) 184–201.
[24] M. Zhao, B. Song, J. Pu, T. Wada, B. Reid, G. Tai, F. Wang, A. Guo, P. Walczysko, Y. Gu, Electrical signals control wound healing through phosphatidylinositol-3-OH kinase-γ and PTEN, Nature. 442 (2006) 457.
[25] M. Kranjc, D. Miklavčič, Electric Field Distribution and Electroporation Threshold, in: D. Miklavcic (Ed.), Handb. Electroporation, Springer International Publishing, Cham, 2016: pp. 1–17. https://doi.org/10.1007/978-3-319-26779-1_4-1.

[26] S. Corovic, I. Lackovic, P. Sustaric, T. Sustar, T. Rodic, D. Miklavcic, Modeling of electric field distribution in tissues during electroporation, Biomed. Eng. OnLine. 12 (2013) 16. https://doi.org/10.1186/1475-925X-12-16.
[27] L. Gibot, T. Galbraith, J. Huot, F.A. Auger, A Preexisting Microvascular Network Benefits In Vivo Revascularization of a Microvascularized Tissue-Engineered Skin Substitute, Tissue Eng. Part A. 16 (2010) 3199–3206. https://doi.org/10.1089/ten.tea.2010.0189.
[28] L. Gibot, T. Galbraith, J. Huot, F.A. Auger, Development of a tridimensional microvascularized human skin substitute to study melanoma biology, Clin. Exp. Metastasis. 30 (2013) 83–90. https://doi.org/10.1007/s10585-012-9511-3.
[29] M. Madi, M.-P. Rols, L. Gibot, Efficient In Vitro Electropermeabilization of Reconstructed Human Dermal Tissue, J. Membr. Biol. 248 (2015) 903–908. https://doi.org/10.1007/s00232-015-9791-z.
[30] A. Figarol, L. Gibot, M. Golzio, B. Lonetti, A.-F. Mingotaud, M.-P. Rols, A journey from the endothelium to the tumor tissue: distinct behavior between PEO-PCL micelles and polymersomes nanocarriers, Drug Deliv. 25 (2018) 1766–1778. https://doi.org/10.1080/10717544.2018.1510064.
[31] L. Gibot, L. Wasungu, J. Teissié, M.-P. Rols, Antitumor drug delivery in multicellular spheroids by electropermeabilization, J. Controlled Release. 167 (2013) 138–147. https://doi.org/10.1016/j.jconrel.2013.01.021.
[32] P.K. Davis, A. Ho, S.F. Dowdy, Biological Methods for Cell-Cycle Synchronization of Mammalian Cells, BioTechniques. 30 (2001) 1322–1331. https://doi.org/10.2144/01306rv01.
[33] L.D. Zorova, V.A. Popkov, E.Y. Plotnikov, D.N. Silachev, I.B. Pevzner, S.S. Jankauskas, V.A. Babenko, S.D. Zorov, A.V. Balakireva, M. Juhaszova, S.J. Sollott, D.B. Zorov, Mitochondrial membrane potential, Anal. Biochem. 552 (2018) 50–59. https://doi.org/10.1016/j.ab.2017.07.009.
[34] K.M. Robinson, M.S. Janes, J.S. Beckman, The selective detection of mitochondrial superoxide by live cell imaging, Nat. Protoc. 3 (2008) 941–947. https://doi.org/10.1038/nprot.2008.56.
[35] J. Zielonka, J. Vasquez-Vivar, B. Kalyanaraman, Detection of 2-hydroxyethidium in cellular systems: a unique marker product of superoxide and hydroethidine, Nat. Protoc. 3 (2008) 8–21. https://doi.org/10.1038/nprot.2007.473.
[36] J.E.N. Jonkman, J.A. Cathcart, F. Xu, M.E. Bartolini, J.E. Amon, K.M. Stevens, P. Colarusso, An introduction to the wound healing assay using live-cell microscopy, Cell Adhes. Migr. 8 (2014) 440–451. https://doi.org/10.4161/cam.36224.
[37] E. Phez, L. Gibot, M.-P. Rols, How transient alterations of organelles in mammalian cells submitted to electric field may explain some aspects of gene electrotransfer process, Bioelectrochemistry. 112 (2016) 166–172. https://doi.org/10.1016/j.bioelechem.2016.02.004.
[38] L.D. Zorova, V.A. Popkov, E.Y. Plotnikov, D.N. Silachev, I.B. Pevzner, S.S. Jankauskas, V.A. Babenko, S.D. Zorov, A.V. Balakireva, M. Juhaszova, S.J. Sollott, D.B. Zorov, Mitochondrial membrane potential, Mitochondrial Biochem. Bioenergenetics. 552 (2018) 50–59. https://doi.org/10.1016/j.ab.2017.07.009.
[39] R.H.W. Funk, Endogenous electric fields as guiding cue for cell migration, Front. Physiol. 6 (2015) 143–143. https://doi.org/10.3389/fphys.2015.00143.
[40] M.S. Kim, M.H. Lee, B.-J. Kwon, M.-A. Koo, G.M. Seon, J.-C. Park, Golgi polarization plays a role in the directional migration of neonatal dermal fibroblasts induced by the direct current electric fields, Biochem. Biophys. Res. Commun. 460 (2015) 255–260. https://doi.org/10.1016/j.bbrc.2015.03.021.
[41] A. Guo, B. Song, B. Reid, Y. Gu, J.V. Forrester, C.A.B. Jahoda, M. Zhao, Effects of Physiological Electric Fields on Migration of Human Dermal Fibroblasts, J. Invest. Dermatol. 130 (2010) 2320–2327. https://doi.org/10.1038/jid.2010.96.
[42] K.S. Fang, E. Ionides, G. Oster, R. Nuccitelli, R.R. Isseroff, Epidermal growth factor receptor relocalization and kinase activity are necessary for directional migration of keratinocytes in DC electric fields, J. Cell Sci. 112 (Pt 12) (1999) 1967–1978.

[43] M. Zhao, J. Pu, J.V. Forrester, C.D. McCaig, Membrane lipids, EGF receptors, and intracellular signals co-localize and are polarized in epithelial cells moving directionally in a physiological electric field, FASEB J. 16 (2002). https://doi.org/10.1096/fj.01-0811fje.
[44] C.E. Pullar, B.S. Baier, Y. Kariya, A.J. Russell, B.A.J. Horst, M.P. Marinkovich, R.R. Isseroff, beta4 integrin and epidermal growth factor coordinately regulate electric field-mediated directional migration via Rac1, Mol. Biol. Cell. 17 (2006) 4925–4935. https://doi.org/10.1091/mbc.e06-05-0433.
[45] G.J. Bourguignon, L.Y. Bourguignon, Electric stimulation of protein and DNA synthesis in human fibroblasts., FASEB J. 1 (1987) 398–402. https://doi.org/10.1096/fasebj.1.5.3678699.
[46] C. Dunnill, T. Patton, J. Brennan, J. Barrett, M. Dryden, J. Cooke, D. Leaper, N.T. Georgopoulos, Reactive oxygen species (ROS) and wound healing: the functional role of ROS and emerging ROS-modulating technologies for augmentation of the healing process, Int. Wound J. 14 (2017) 89–96. https://doi.org/10.1111/iwj.12557.
[47] J. Kanta, The role of hydrogen peroxide and other reactive oxygen species in wound healing, Acta Medica (Hradec Kralove). 54 (2011) 97–101.
[48] B. Gabriel, J. Teissie, Generation of reactive-oxygen species induced by electropermeabilization of Chinese hamster ovary cells and their consequence on cell viability, Eur. J. Biochem. 223 (1994) 25–33.
[49] P. Bonnafous, M.-C. Vernhes, J. Teissié, B. Gabriel, The generation of reactive-oxygen species associated with long-lasting pulse-induced electropermeabilisation of mammalian cells is based on a non-destructive alteration of the plasma membrane, Biochim. Biophys. Acta BBA-Biomembr. 1461 (1999) 123–134.
[50] M. Breton, L.M. Mir, Investigation of the chemical mechanisms involved in the electropulsation of membranes at the molecular level, Bioelectrochemistry. 119 (2018) 76–83.
[51] T. Kotnik, L. Rems, M. Tarek, D. Miklavčič, Membrane Electroporation and Electropermeabilization: Mechanisms and Models, Annu. Rev. Biophys. 48 (2019) 63–91. https://doi.org/10.1146/annurev-biophys-052118-115451.
[52] I.V. Klyubin, K.M. Kirpichnikova, I.A. Gamaley, Hydrogen peroxide-induced chemotaxis of mouse peritonecul neutrophils, (1996).
[53] M.M. Shi, J.J. Godleski, J.D. Paulauskis, Regulation of macrophage inflammatory protein-1 mRNA by oxidative stress, J. Biol. Chem. 271 (1996) 5878–5883.
[54] J.R. Stone, T. Collins, The role of hydrogen peroxide in endothelial proliferative responses, Endothelium. 9 (2002) 231–238.
[55] P.A. Hyslop, D.B. Hinshaw, I.U. Scraufstatter, C.G. Cochrane, S. Kunz, K. Vosbeck, Hydrogen peroxide as a potent bacteriostatic antibiotic: implications for host defense, Free Radic. Biol. Med. 19 (1995) 31–37.
[56] M. Schäfer, S. Werner, Oxidative stress in normal and impaired wound repair, Pharmacol. Res. 58 (2008) 165–171.
[57] R. Moseley, J.E. Stewart, P. Stephens, R.J. Waddington, D.W. Thomas, Extracellular matrix metabolites as potential biomarkers of disease activity in wound fluid: lessons learned from other inflammatory diseases?, Br. J. Dermatol. 150 (2004) 401–413.
[58] Y. Gu, J. Han, C. Jiang, Y. Zhang, Biomarkers, oxidative stress and autophagy in skin aging, Ageing Res. Rev. (2020) 101036.
[59] S. Yoshimoto, N. Kohara, N. Sato, H. Ando, M. Ichihashi, Riboflavin Plays a Pivotal Role in the UVA-Induced Cytotoxicity of Fibroblasts as a Key Molecule in the Production of H2O2 by UVA Radiation in Collaboration with Amino Acids and Vitamins, Int. J. Mol. Sci. 21 (2020) 554.
[60] D.R. Maldaner, V.F. Azzolin, F. Barbisan, M.H. Mastela, C.F. Teixeira, A. Dihel, T. Duarte, N.L. Pellenz, L.F.C. Lemos, C.M.U. Negretto, In vitro effect of low-level laser therapy on the proliferative, apoptosis modulation, and oxi-inflammatory markers of premature-senescent hydrogen peroxide-induced dermal fibroblasts, Lasers Med. Sci. 34 (2019) 1333–1343.

[61] C.Y. Calvet, D. Famin, F.M. André, L.M. Mir, Electrochemotherapy with bleomycin induces hallmarks of immunogenic cell death in murine colon cancer cells, Oncoimmunology. 3 (2014) e28131.
[62] G. Kroemer, L. Galluzzi, O. Kepp, L. Zitvogel, Immunogenic Cell Death in Cancer Therapy, Annu. Rev. Immunol. 31 (2013) 51–72. https://doi.org/10.1146/annurev-immunol-032712-100008.
[63] L.B. Nanney, C.D. Woodrell, M.R. Greives, N.L. Cardwell, A.C. Pollins, T.A. Bancroft, A. Chesser, M. Michalak, M. Rahman, J.W. Siebert, Calreticulin enhances porcine wound repair by diverse biological effects, Am. J. Pathol. 173 (2008) 610–630.
[64] E. Gendaszewska-Darmach, M. Kucharska, Nucleotide receptors as targets in the pharmacological enhancement of dermal wound healing, Purinergic Signal. 7 (2011) 193. https://doi.org/10.1007/s11302-011-9233-z.
[65] A.S. Torres, A. Caiafa, A.L. Garner, S. Klopman, N. LaPlante, C. Morton, K. Conway, A.D. Michelson, A.L.I. Frelinger, V.B. Neculaes, Platelet activation using electric pulse stimulation: Growth factor profile and clinical implications, J. Trauma Acute Care Surg. 77 (2014) S94. https://doi.org/10.1097/TA.0000000000000322.
[66] A.L. Frelinger 3rd, A.J. Gerrits, V.B. Neculaes, T. Gremmel, A.S. Torres, A. Caiafa, S.L. Carmichael, A.D. Michelson, Tunable activation of therapeutic platelet-rich plasma by pulse electric field: Differential effects on clot formation, growth factor release, and platelet morphology, PloS One. 13 (2018) e0203557–e0203557. https://doi.org/10.1371/journal.pone.0203557.
[67] A. Prevc, A. Bedina Zavec, M. Cemazar, V. Kloboves-Prevodnik, M. Stimac, V. Todorovic, P. Strojan, G. Sersa, Bystander Effect Induced by Electroporation is Possibly Mediated by Microvesicles and Dependent on Pulse Amplitude, Repetition Frequency and Cell Type, J. Membr. Biol. 249 (2016) 703–711. https://doi.org/10.1007/s00232-016-9915-0.
[68] F. Pampaloni, E.G. Reynaud, E.H.K. Stelzer, The third dimension bridges the gap between cell culture and live tissue, Nat. Rev. Mol. Cell Biol. 8 (2007) 839.
[69] B. Marrero, R. Heller, The use of an in vitro 3D melanoma model to predict in vivo plasmid transfection using electroporation, Biomaterials. 33 (2012) 3036–3046. https://doi.org/10.1016/j.biomaterials.2011.12.049.
[70] M. Madi, M.-P. Rols, L. Gibot, Gene Electrotransfer in 3D Reconstructed Human Dermal Tissue, Curr Gene Ther. 16 (2016) 75–82. https://doi.org/10.2174/1566523216666160331125052.
[71] A.A. Bulysheva, N. Burcus, C. Lundberg, C.M. Edelblute, M.P. Francis, R. Heller, Recellularized human dermis for testing gene electrotransfer ex vivo, Biomed. Mater. 11 (2016) 035002.